


## All-optical three-dimensional orientation of asymmetric-top molecules with combined linearly and elliptically polarized two-color laser fields

Md. Maruf Hossain <sup>1,2,\*</sup> Nanse Esaki <sup>1</sup> and Hirofumi Sakai <sup>1,3,†</sup><sup>1</sup>*Department of Physics, Graduate School of Science, The University of Tokyo, 7-3-1 Hongo, Bunkyo-ku, Tokyo 113-0033, Japan*<sup>2</sup>*IBM Research Tokyo, 19-21, Nihonbashi, Hakozi-cho, Chuo-ku, Tokyo 103-8510, Japan*<sup>3</sup>*Institute for Photon Science and Technology, Graduate School of Science, The University of Tokyo, 7-3-1 Hongo, Bunkyo-ku, Tokyo 113-0033, Japan* (Received 18 August 2023; revised 22 October 2023; accepted 16 November 2023; published 26 December 2023)

We propose an approach to the realization of all-optical three-dimensional molecular orientation, in which a linearly polarized fundamental pulse and an elliptically polarized second-harmonic pulse with one of the polarization axes parallel to the linear polarization of the fundamental pulse are employed to orient asymmetric-top molecules, leading to higher degrees of orientation. In addition to the one-dimensional orientation realized along the linearly polarized fundamental pulse, planar molecular alignment can be naturally realized along the elliptical polarization plane of the second-harmonic pulse, resulting in the three-dimensional molecular orientation. Compared to another all-optical method to achieve three-dimensional molecular orientation, in which linearly polarized two-color laser fields with their polarizations crossed obliquely are employed, it is numerically demonstrated that our method with an elliptically polarized second-harmonic pulse is especially advantageous when the molecular orientation dynamics is nonadiabatic.

DOI: [10.1103/PhysRevA.108.063109](https://doi.org/10.1103/PhysRevA.108.063109)

### I. INTRODUCTION

A sample of aligned and oriented molecules is an ideal anisotropic quantum system to investigate electronic stereodynamics in molecules [1] as well as stereodynamics in chemical reactions. Therefore, the developments of various molecular alignment and orientation techniques with laser technologies are one of the hot topics in molecular science over the last quarter century [2,3]. When molecules are aligned, they are parallel to each other without paying any attention to the head-versus-tail order. In contrast, when molecules are oriented, they are parallel to each other with their heads directed the same way as much as possible quantum mechanically. Typical applications of a sample of aligned and oriented molecules are summarized in Ref. [4]. They are tunnel ionization [5], nonsequential double ionization [6], control of multiphoton ionization [7], high-order harmonic generation [8,9], and so on. Some recent applications include the shooting of molecular movies based on ultrafast x-ray electron diffraction [10,11] and the control of pendular qubit states [12]. As is naturally expected, the realization of molecular orientation is much more challenging than that of molecular alignment. The molecular alignment techniques are well established and used in many applications [4].

The development of the molecular orientation technique first comes with the so-called combined-field technique [13,14], in which a weak electrostatic field and an intense nonresonant laser field are employed to achieve molecular

orientation. In the early stage, one- [15,16] and three-dimensional molecular orientation [17] and laser-field-free molecular orientation [18] were achieved. Then after the realization of laser-field-free orientation of state-selected asymmetric-top (iodobenzene) molecules [19], laser-field-free three-dimensional molecular orientation [20] was achieved, and that can be regarded as the acme of the combined-field technique because all three requirements desired for molecular orientation techniques, that is, higher degrees of orientation, laser-field-free condition, and three-dimensional control of spatial direction of sample molecules corresponding to the complete control of spatial direction of sample molecules, were successfully fulfilled.

Another promising approach is all-optical molecular orientation with intense nonresonant two-color laser fields, which relies on the anisotropic hyperpolarizability interaction as well as anisotropic polarizability interaction [21]. The proof-of-principle experiment was reported in 2010 [22]. More recently, stronger orientation of state-selected OCS molecules was achieved by relative-delay-adjusted nanosecond two-color laser pulses [23]. Here it must be noted that the highest possible degrees of molecular orientation for given laser intensities can be achieved when the molecular orientation dynamics is purely adiabatic. Our numerical simulations suggest that longer pulses are necessary to ensure that the molecular orientation dynamics is adiabatic for the all-optical molecular orientation technique than for the combined-field technique [24–26]. In the course of the enormous efforts to increase the degrees of molecular orientation after the proof-of-principle experiment [22], it has been revealed that the molecular orientation dynamics is not adiabatic even with 10-ns two-color laser pulses [12]. In order to mitigate the disadvantage

\*maruf@light.phys.s.u-tokyo.ac.jp

†hsakai@phys.s.u-tokyo.ac.jp

associated with the nonadiabaticity in the molecular orientation dynamics, some approaches have been proposed [27–29].

Among those approaches, our approach with a linearly polarized fundamental ( $\omega$ ) pulse and an elliptically polarized second-harmonic ( $2\omega$ ) pulse [29] was originally devised to increase the degree of molecular orientation when the molecular orientation dynamics is nonadiabatic. By carefully examining various combinations of the polarization states of the two wavelengths, we have found that the specific combination of a linearly polarized  $\omega$  pulse and an elliptically polarized  $2\omega$  pulse is the most effective to increase the degree of molecular orientation [29]. Since the molecular plane can be confined to the elliptical polarization plane of the  $2\omega$  pulse, our approach should be applicable to achieve three-dimensional molecular orientation of asymmetric-top molecules such as iodobenzene molecules. In this paper, we demonstrate that our approach can be naturally extended to achieve three-dimensional molecular orientation by showing all the order parameters to characterize three-dimensional molecular orientation can be successfully controlled. We also show that, in order to achieve three-dimensional molecular orientation, our approach is superior to another approach using linearly polarized two-color laser pulses with their polarizations crossed obliquely [30] especially when the molecular orientation dynamics is nonadiabatic.

In this connection, all-optical field-free three-dimensional orientation of asymmetric-top molecules is demonstrated by means of phase-locked cross-polarized two-color laser pulses [31]. Since intense femtosecond two-color pulses are used in their experiment, the molecular orientation dynamics is purely nonadiabatic, and an ensemble of field-free molecules is created after the two-color pulses are over. Consequently, the degree of molecular orientation is very low, and the absolute value of the standard molecular orientation parameter is  $\approx 0.05$ . In addition, in their approach, the relative intensities of the femtosecond two-color pulses must be carefully chosen depending on the specific sample molecule. In contrast, our approach is less sensitive to the relative intensities of nanosecond two-color laser pulses as discussed below. As for other experimental studies on molecular orientation with intense femtosecond two-color pulses, the readers should refer to the Introduction of Ref. [26].

## II. DEFINITIONS OF TWO-COLOR LASER FIELDS

First, for comparison, linearly polarized two-color laser fields with their polarizations crossed obliquely are defined as follows [30]:

$$\begin{bmatrix} E_X(t) \\ E_Y(t) \\ E_Z(t) \end{bmatrix} = \begin{bmatrix} E'_{2\omega}(t) \cos(2\omega t + \Phi) \\ 0 \\ E_\omega(t) \cos \omega t + E_{2\omega}(t) \cos(2\omega t + \Phi) \end{bmatrix}, \quad (1)$$

where  $\omega$  and  $2\omega$  are the angular frequencies of the fundamental ( $\omega$ ) pulse and its second-harmonic ( $2\omega$ ) pulse, respectively;  $\Phi$  is the relative phase difference between the two wavelengths; and the envelopes  $E_\omega(t)$ ,  $E_{2\omega}(t)$ , and  $E'_{2\omega}(t)$  are

defined as Gaussian pulses:

$$\begin{aligned} E_\omega(t) &= E_\omega e^{-\frac{t^2}{2\tau_\omega^2}}, \\ E_{2\omega}(t) &= E_{2\omega} e^{-\frac{t^2}{2\tau_{2\omega}^2}}, \quad E'_{2\omega}(t) = E'_{2\omega} e^{-\frac{t^2}{2\tau_{2\omega}^2}}, \end{aligned} \quad (2)$$

where  $\tau_\omega$  and  $\tau_{2\omega}$  are the widths of the Gaussian envelopes. The polarizations and the propagation directions of the two-color laser fields are defined in the laboratory-fixed frame as shown in Fig. 1(a), while the body-fixed frame of a sample (iodobenzene) molecule is defined in Fig. 1(b).  $\mathbf{e}_Y$  and  $\mathbf{e}_y$  are the unit vectors along the laboratory-fixed  $Y$  axis and the body-fixed  $y$  axis, respectively. In Eq. (2),  $E_\omega$  is the peak electric-field strength of the  $\omega$  pulse, and  $E_{2\omega}$  and  $E'_{2\omega}$  are those projected along the  $Z$  and  $X$  axis of the linearly polarized  $2\omega$  pulse, respectively. In this paper, we refer to the  $Z$  axis as the vertical direction and to the  $X$  axis as the horizontal direction. The transformation from the laboratory-fixed frame to the body-fixed frame of a sample molecule is expressed by the Euler angles  $\phi$ ,  $\theta$ , and  $\chi$  as shown in Fig. 1(c). We express the Hamiltonians of the rotational dynamics in the body-fixed frame of the molecule.

In our approach, we replace the linearly polarized  $2\omega$  pulse with an *elliptically* polarized one:

$$\begin{bmatrix} E_X(t) \\ E_Y(t) \\ E_Z(t) \end{bmatrix} = \begin{bmatrix} E'_{2\omega}(t) \sin(2\omega t + \Phi) \\ 0 \\ E_\omega(t) \cos \omega t + E_{2\omega}(t) \cos(2\omega t + \Phi) \end{bmatrix}, \quad (3)$$

where  $E_{2\omega}(t)$  and  $E'_{2\omega}(t)$  are the peak electric-field strengths along the  $Z$  and  $X$  axis of the elliptically polarized  $2\omega$  pulse, respectively. Note that a cosine function of the  $X$  component in Eq. (1) is now replaced by a sine function in Eq. (3). Here we assume that the two-color laser fields oscillate much faster than the rotational period of the molecules, and the conditions  $\omega/2\pi \gg \tau_\omega^{-1}$  and  $2\omega/2\pi \gg \tau_{2\omega}^{-1}$ , allowing us to take the average over a laser oscillation period  $2\pi/\omega$  when considering the effective laser-molecule interaction potentials responsible for rotational control of molecules with (two-color) laser fields [21,25,29,33]. In addition, the combination of the  $\omega$  pulse and the  $2\omega$  pulse is essential for achieving molecular orientation [29,34]. Since the all-optical molecular orientation technique considered here relies on the nonresonant laser-molecule interaction, we do not have to specify the two wavelengths (angular frequencies).

## III. INTERACTION POTENTIALS

We will consider *rigid* asymmetric-top molecules such as iodobenzene ( $C_6H_5I$ ) which belongs to the point group  $C_{2v}$  [35–37]. The reason why an iodobenzene ( $C_6H_5I$ ) is used as a typical sample molecule in the present paper is to mitigate the calculation cost. In general, the numerical calculations of three-dimensional alignment and orientation are very time consuming, especially when solving time-dependent Schrödinger equations. Since an iodobenzene molecule which belongs to the point group  $C_{2v}$  has four symmetry operations, the number of nonzero matrix elements to be included in the calculations can be considerably reduced, leading to the fairly large reduction of the calculation time. First, the interaction

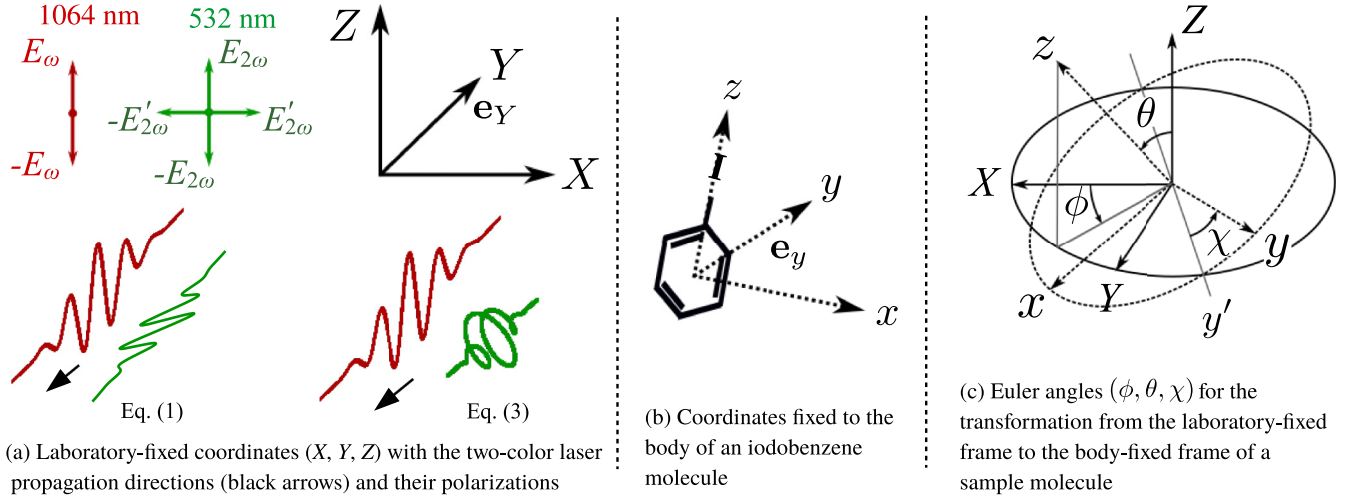


FIG. 1. (a) The polarizations and the propagation directions of the two-color laser fields are defined in the laboratory-fixed frame. (b) The body-fixed frame of a sample (iodobenzene) molecule.  $e_y$  and  $e_y$  are the unit vectors along the laboratory-fixed Y axis and the body-fixed y axis, respectively. (c) The transformation from the laboratory-fixed frame to the body-fixed frame of a sample molecule is expressed by the Euler angles  $\phi$ ,  $\theta$ , and  $\chi$ , and is achieved by three successive finite rotations: a counterclockwise rotation  $\phi$  about Z, a counterclockwise rotation  $\theta$  about the line of nodes  $y'$ , and a counterclockwise rotation  $\chi$  about  $z$  [32].

potentials (Hamiltonians) of the asymmetric-top molecule (iodobenzene) with linearly polarized two-color laser fields with their polarizations crossed obliquely as in Eq. (1) [30] are given by

$$\hat{H}_i = \hat{H}_\alpha + \hat{H}_\beta, \quad (4)$$

$$\begin{aligned} \hat{H}_\alpha = & -\frac{1}{4}\alpha^{xy}(\cos\phi\cos\theta\cos\chi - \sin\phi\sin\chi)^2 E_{2\omega}^2(t) \\ & -\frac{1}{4}\alpha^{xy}\sin^2\theta\cos^2\chi[E_\omega^2(t) + E_{2\omega}^2(t)] \\ & +\frac{1}{2}\alpha^{xy}\sin\theta\cos\chi(\cos\phi\cos\theta\cos\chi \\ & -\sin\phi\sin\chi)E_{2\omega}(t)E'_{2\omega}(t) \\ & -\frac{1}{4}\alpha^{zy}\cos^2\phi\sin^2\theta E_{2\omega}^2(t) \\ & -\frac{1}{4}\alpha^{zy}\cos^2\theta[E_\omega^2(t) + E_{2\omega}^2(t)] \\ & -\frac{1}{2}\alpha^{zy}\cos\phi\cos\theta\sin\theta E_{2\omega}(t)E'_{2\omega}(t), \end{aligned} \quad (5)$$

$$\begin{aligned} \hat{H}_\beta = & \cos\Phi \left\{ -\frac{3}{8}\beta_{zxx}\cos\theta\sin^2\theta\cos^2\chi E_\omega^2(t)E_{2\omega}(t) \right. \\ & -\frac{1}{8}\beta_{zxx}[\cos\phi\sin\theta(1-3\cos^2\theta)\cos^2\chi \\ & +\sin\phi\cos\theta\sin\theta\sin 2\chi]E_\omega^2(t)E'_{2\omega}(t) \\ & -\frac{3}{8}\beta_{zyy}\cos\theta\sin^2\theta\sin^2\chi E_\omega^2(t)E_{2\omega}(t) \\ & -\frac{1}{8}\beta_{zyy}[\cos\phi\sin\theta(1-3\cos^2\theta)\sin^2\chi \\ & -\sin\phi\cos\theta\sin\theta\sin 2\chi]E_\omega^2(t)E'_{2\omega}(t) \\ & -\frac{1}{8}\beta_{zzz}\cos^3\theta E_\omega^2(t)E_{2\omega}(t) \\ & \left. -\frac{1}{8}\beta_{zzz}\cos\phi\cos^2\theta\sin\theta E_\omega^2(t)E'_{2\omega}(t) \right\}. \end{aligned} \quad (6)$$

The phase difference between the two wavelengths is set to be  $\Phi = 0$  or  $\pi$ ,  $\alpha_{ij}$  and  $\beta_{ijk}$  are the polarizability and hyperpolarizability tensor components, and  $\alpha^{zy} = \alpha_{zz} - \alpha_{yy} \neq \alpha_{zy}$  and  $\alpha^{xy} = \alpha_{xx} - \alpha_{yy} \neq \alpha_{xy}$ . The body-fixed coordinates  $x$ ,  $y$ , and  $z$  are defined in Fig. 1(b). The above interaction potentials [Eqs. (5) and (6)] are derived after taking the average over a

laser oscillation period  $2\pi/\omega$ . The potential  $\hat{H}_\alpha$  is created by the anisotropic polarizability interaction and the potential  $\hat{H}_\beta$  is created by the anisotropic hyperpolarizability interaction. Since the potential  $\hat{H}_\alpha$  is invariant under the transformation [32]  $\phi \rightarrow \pi + \phi$ ,  $\theta \rightarrow \pi - \theta$ ,  $\chi \rightarrow -\chi$ , i.e.,  $\hat{H}_\alpha(\phi, \theta, \chi) = \hat{H}_\alpha(\pi + \phi, \pi - \theta, -\chi)$ , no orientation is produced when only the polarizability interaction potential is considered. On the other hand, the anisotropic hyperpolarizability interaction potential  $\hat{H}_\beta$  has the opposite sign under the above transformation, i.e.,  $\hat{H}_\beta(\phi, \theta, \chi) = -\hat{H}_\beta(\pi + \phi, \pi - \theta, -\chi)$ , being responsible for molecular orientation.

For linearly polarized two-color laser fields with their polarizations crossed obliquely, the  $\hat{H}_\alpha$  for the molecular parameters of an iodobenzene molecule (Table I) is plotted in terms of the Euler angles  $\phi$ ,  $\theta$ , and  $\chi$  in Fig. 2, in which  $\Phi = 0$  is assumed. The potentials plotted in Fig. 2 are those at the peak intensities of the two-color laser pulses as given in Table II. It is experimentally feasible to have  $2\omega$  intensity that equals or exceeds the  $\omega$  intensity by using an attenuator for the  $\omega$  pulse, consisting of the combination of a dual wavelength half waveplate and a polarizer. The peak intensity  $I$  and its corresponding peak electric-field strength  $E$  are related by  $I = E^2/2Z_0$  with the characteristic impedance of vacuum  $Z_0$ .

One can see that the  $\hat{H}_\alpha$  has its minimum deviated from the vertical Z axis. This further means that the asymmetric-top molecules can be aligned tilted from the vertical Z axis

TABLE I. Rotational constants, polarizability, and hyperpolarizability components of an iodobenzene molecule.

	Rotational constants (J) [36,37]	Polarizability ( $\text{C}^2 \text{m}^2 \text{J}^{-1}$ ) [35]	Hyperpolarizability ( $\text{C}^3 \text{m}^3 \text{J}^{-2}$ ) [35]
A	$3.76 \times 10^{-24}$	$\alpha_{zz}$ $2.39 \times 10^{-39}$	$\beta_{zzz}$ $1.44 \times 10^{-50}$
B	$4.97 \times 10^{-25}$	$\alpha_{xx}$ $1.63 \times 10^{-39}$	$\beta_{zxx}$ $3.49 \times 10^{-52}$
C	$4.39 \times 10^{-25}$	$\alpha_{yy}$ $1.01 \times 10^{-39}$	$\beta_{zyy}$ $2.2 \times 10^{-51}$

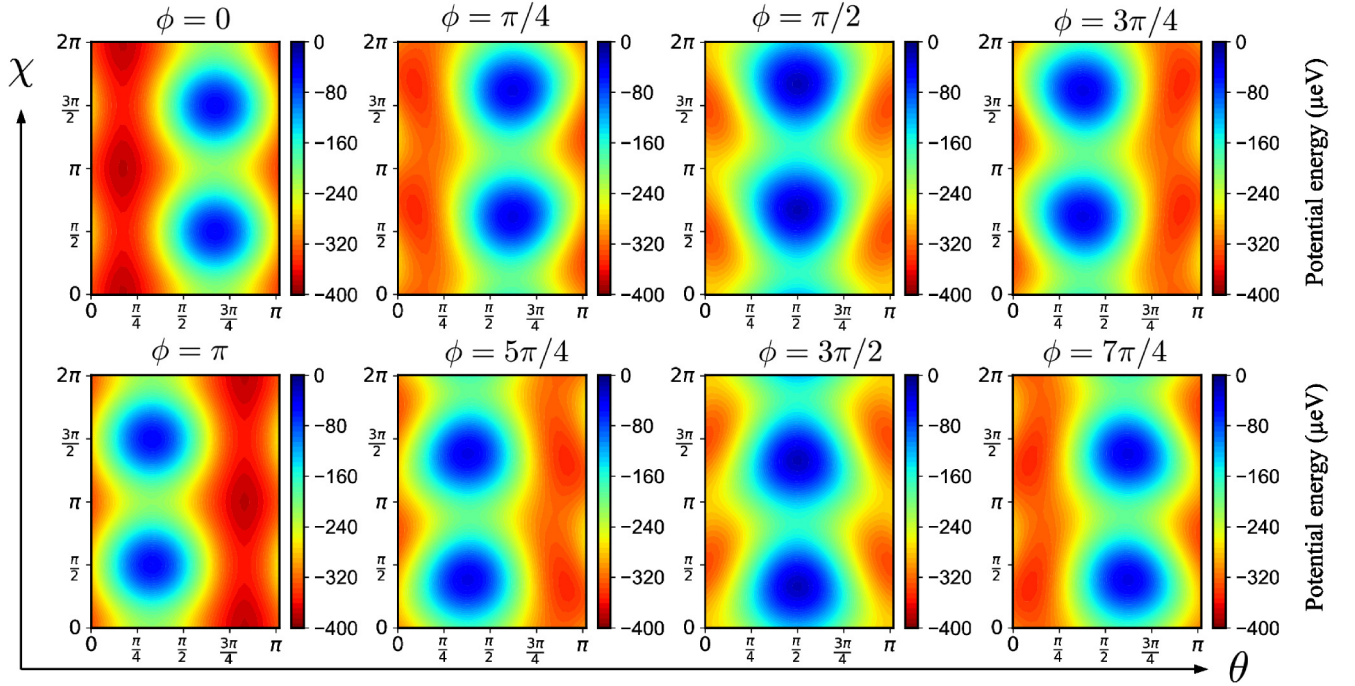


FIG. 2. Alignment potential  $\hat{H}_\alpha$  as a function of  $\phi$ ,  $\theta$ , and  $\chi$ , in which linearly polarized two-color laser fields with their polarizations crossed obliquely are employed to orient iodobenzene molecules. The relative phase  $\Phi$  between the two wavelengths is assumed to be zero.

depending on the contribution of the  $E'_{2\omega}(t)$ . The potential  $\hat{H}_\beta$  given by Eq. (6) is shown in Fig. 3. In contrast to  $\hat{H}_\alpha$ , the potential  $\hat{H}_\beta$  is the deepest at  $\theta \approx 0$  for all values of the Euler angle  $\phi$ . The slight deviation of the deepest positions of the potentials  $\hat{H}_\beta$  from the exact  $\theta = 0$  is caused by the terms including  $E'_{2\omega}(t)$  in Eq. (6). Since the potential  $\hat{H}_\alpha$  is much deeper than the potential  $\hat{H}_\beta$  by about three orders of magnitude and dominates the overall shape of the interaction potential, the spatial direction of a sample of oriented molecules is accordingly tilted from the vertical Z axis depending on the contribution of the  $E'_{2\omega}(t)$ .

The interaction potentials of an asymmetric-top molecule and a combined linearly and elliptically polarized two-color laser field defined by Eq. (3) are given by Eqs. (7)–(9):

$$\hat{H}_i = \hat{H}_\alpha + \hat{H}_\beta, \quad (7)$$

$$\begin{aligned} \hat{H}_\alpha = & -\frac{1}{4}\alpha^{xy}(\cos\phi\cos\theta\cos\chi - \sin\phi\sin\chi)^2 E_{2\omega}^2(t) \\ & -\frac{1}{4}\alpha^{xy}\sin^2\theta\cos^2\chi[E_\omega^2(t) + E_{2\omega}^2(t)] \\ & -\frac{1}{4}\alpha^{zy}\cos^2\phi\sin^2\theta E_{2\omega}^2(t) \\ & -\frac{1}{4}\alpha^{zy}\cos^2\theta[E_\omega^2(t) + E_{2\omega}^2(t)], \end{aligned} \quad (8)$$

TABLE II. Peak intensities of the two-color laser pulses.

Laser field	Intensity (W/cm <sup>2</sup> )
Fundamental pulse (vertical direction), $I_\omega$	$8 \times 10^9$
Second harmonic (vertical direction), $I_{2\omega}$	$9 \times 10^9$
Second harmonic (horizontal direction), $I'_{2\omega}$	$8 \times 10^9$

$$\begin{aligned} \hat{H}_\beta = & \cos\Phi \left[ -\frac{3}{8}\beta_{zxx}\cos\theta\sin^2\theta\cos^2\chi E_\omega^2(t)E_{2\omega}(t) \right. \\ & -\frac{3}{8}\beta_{zyy}\cos\theta\sin^2\theta\sin^2\chi E_\omega^2(t)E_{2\omega}(t) \\ & \left. -\frac{1}{8}\beta_{zzz}\cos^3\theta E_\omega^2(t)E_{2\omega}(t) \right], \end{aligned} \quad (9)$$

where  $\Phi = 0$  or  $\pi$  as in Eqs. (4)–(6). The elliptically polarized  $2\omega$  pulse defined by Eq. (3) makes the terms associated with  $E_{2\omega}(t)E'_{2\omega}(t)$  in  $\hat{H}_\alpha$  and  $E_\omega^2(t)E'_{2\omega}(t)$  in  $\hat{H}_\beta$  zero after taking the average over the laser oscillation period  $2\pi/\omega$ . In this case, molecular orientation can be achieved either upward ( $\theta \approx 0$ ) or downward ( $\theta \approx \pi$ ) by tuning the relative phase  $\Phi$  between the two wavelengths, except for the extreme case in which  $E'_{2\omega}(t)$  is much higher than  $E_{2\omega}(t)$ , approaching the case proposed in Ref. [28], in contrast to the linearly polarized two-color laser fields with their polarizations crossed obliquely.

The polarizability interaction potential  $\hat{H}_\alpha$  for the molecular parameters of an iodobenzene molecule (Table I) is plotted in terms of the Euler angles  $\phi$ ,  $\theta$ , and  $\chi$  in Fig. 4, in which  $\Phi = 0$  is assumed. Our approach is robust to the relative intensities between the two wavelengths as long as the intensities of the two wavelengths are more or less of the same order. In addition, although our enormous auxiliary calculations suggest that the ratio  $I'_{2\omega}/I_{2\omega} \approx 1$  is generally advantageous, as has been originally proposed in Ref. [29], the polarization of the  $2\omega$  pulse does not have to be circular. In contrast to the results shown in Fig. 2 for linearly polarized two-color laser fields with their polarizations crossed obliquely, the potential  $\hat{H}_\alpha$  has its minimum along the vertical Z axis. The hyperpolarizability interaction potential  $\hat{H}_\beta$  is plotted in Fig. 5. Since the terms including  $E_\omega^2(t)E'_{2\omega}(t)$  in  $\hat{H}_\beta$  become



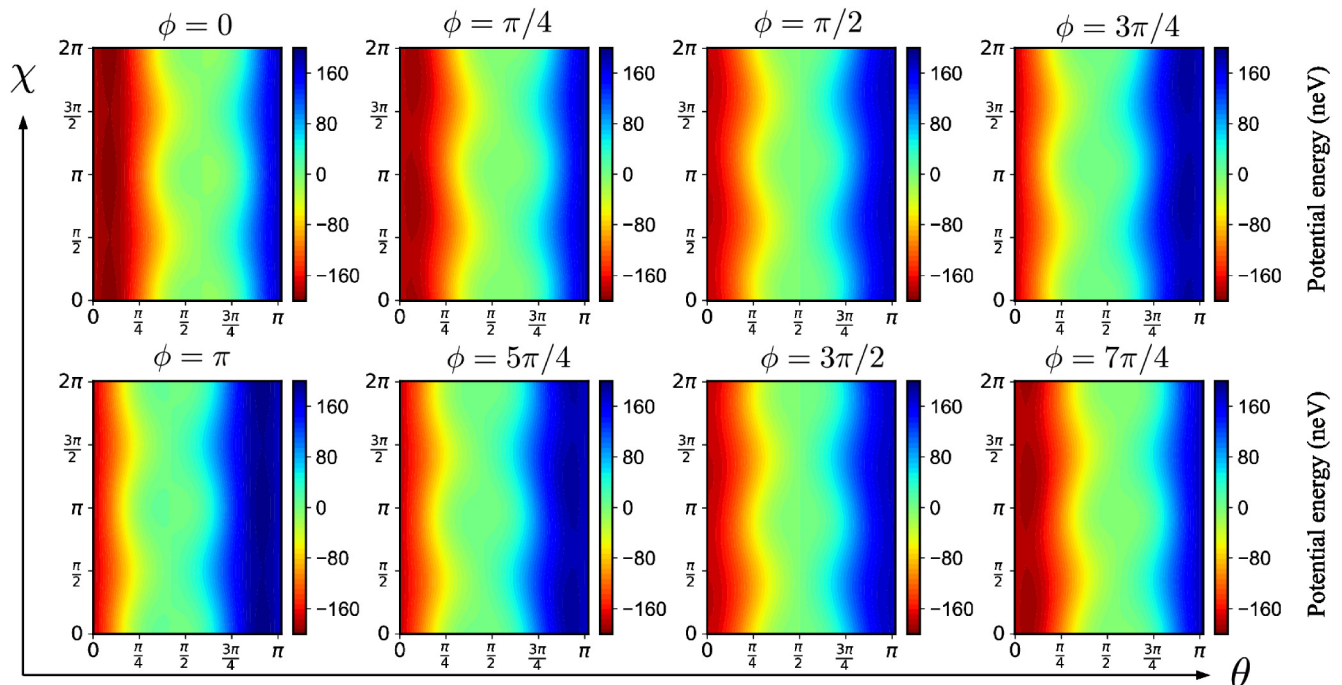


FIG. 3. Orientation potential  $\hat{H}_\beta$  as a function of  $\phi$ ,  $\theta$ , and  $\chi$ , in which linearly polarized two-color laser fields with their polarizations crossed obliquely are employed to orient iodobenzene molecules. The relative phase  $\Phi$  between the two wavelengths is assumed to be zero.

zero after taking the cycle average, the hyperpolarizability interaction potential  $\hat{H}_\beta$  is independent of the Euler angle  $\phi$ . Consequently, the spatial direction of a sample of oriented molecules is always along the vertical Z axis, which is very convenient for experimental applications. We would like to emphasize that this superiority in the specific combination

of a linearly polarized  $\omega$  pulse and an elliptically polarized  $2\omega$  pulse over the conventional approach [30] is brought by the avoidance of making the competing spatial direction with a linearly polarized  $\omega$  pulse by employing an elliptically polarized  $2\omega$  pulse instead of a linearly polarized  $2\omega$  pulse.

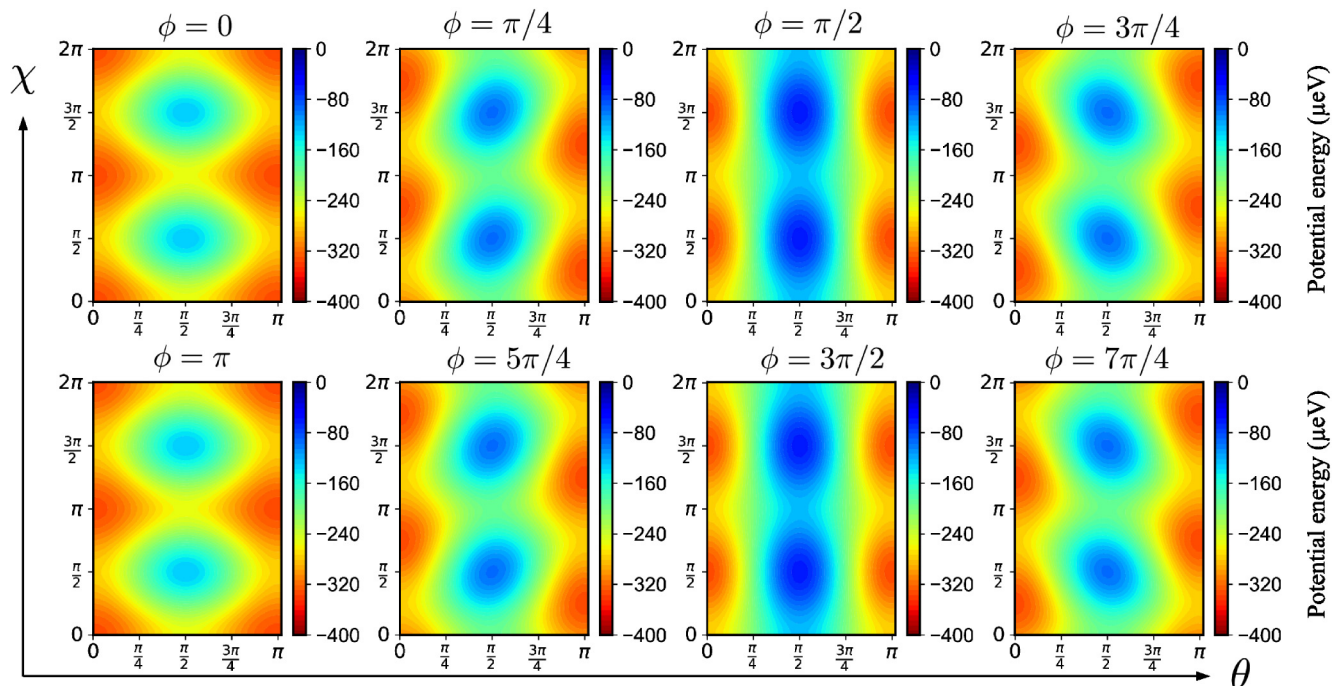


FIG. 4. Alignment potential  $\hat{H}_\alpha$  as a function of  $\phi$ ,  $\theta$ , and  $\chi$ , in which a linearly polarized  $\omega$  pulse and an elliptically polarized  $2\omega$  pulse are employed to orient iodobenzene molecules. The relative phase  $\Phi$  between the two wavelengths is assumed to be zero.

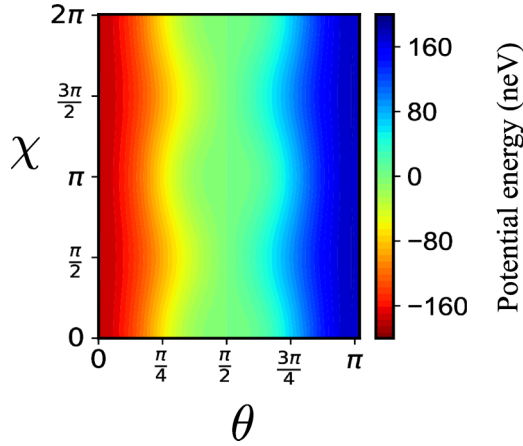


FIG. 5. Orientation potential  $\hat{H}_\beta$  as a function of  $\theta$  and  $\chi$ , in which a linearly polarized  $\omega$  pulse and an elliptically polarized  $2\omega$  pulse are employed to orient iodobenzene molecules. The relative phase  $\Phi$  between the two wavelengths is assumed to be zero.

In addition, the term including the horizontal electric-field component  $E'_{2\omega}(t)$  appears not in  $\hat{H}_\beta$  but in  $\hat{H}_\alpha$ . This leads to an important result that the alignment potential  $\hat{H}_\alpha$  is suppressed along the azimuthal angles  $\phi = 0$  and  $\pi$  without influencing the orientation potential  $\hat{H}_\beta$  (see the plots for  $\phi = 0$  and  $\pi$  in Fig. 4, and Fig. 3 of Ref. [29]). Thereby, the tunnel transition probability from the shallower potential well to the deeper one is increased when the molecular orientation dynamics is nonadiabatic.

#### IV. NUMERICAL SIMULATIONS OF MOLECULAR ORIENTATION DYNAMICS AND DISCUSSIONS

The orientation dynamics of an asymmetric-top (iodobenzene) molecule has been numerically compared between the following two cases.

(1) The time-independent Schrödinger equation is solved under the adiabatic approximation.

(2) The time-dependent Schrödinger equation is solved to take account of the nonadiabatic effects appropriately.

In the numerical calculations, we assume that the iodobenzene molecule is initially in its rotational ground state in the laser-field-free condition. The width  $\tau_\omega$  of the  $\omega$  pulse and the width  $\tau_{2\omega}$  of the  $2\omega$  pulse are  $\tau_\omega = 12$  ns and  $\tau_{2\omega} = 9$  ns, respectively. It should be noted that these pulse widths are about twice those used in our recent experiments [22,23]. These longer pulse widths are intentionally employed to explore the nonadiabaticity of the molecular orientation dynamics as discussed below. As has been discussed in Refs. [24–26], nanosecond two-color laser pulses are much more advantageous for achieving higher degree of orientation than femtosecond two-color laser pulses.

Prior to the results of numerical calculations, we confirm some basic properties of an iodobenzene molecule. The rotational constants and polarizability and hyperpolarizability components are summarized in Table I. The rotational constants meet the condition:  $A > B > C$ , which is equivalent to the relation  $I_a < I_b < I_c$ , where  $I_a$ ,  $I_b$ , and  $I_c$  are the principal moments of inertia along the body-fixed  $z$ ,  $x$ , and  $y$  axes.

As can be seen from Fig. 1(b), iodobenzene molecules belong to the point group  $C_{2v}$  [35–37]. The  $C_2$ -rotational axis falls on the body-fixed  $z$  axis. This axis goes through the iodine atom, which is about an order of magnitude heavier than carbon atoms. Therefore, the principal moment of inertia axis  $a$  also falls on the body-fixed  $z$  axis. According to the right-hand rule of vector product, the principal moment of inertia axes  $b$  and  $c$  correspond to the body-fixed  $x$  and  $y$  axes. Then we explain a way of characterizing the degree of three-dimensional orientation of asymmetric-top molecules. To that end, it is necessary to use three order parameters; i.e., in addition to the usual order parameters of alignment  $\langle \cos^2 \theta \rangle$  and orientation  $\langle \cos \theta \rangle$  measured from the space-fixed vertical  $Z$  axis defined by the linearly polarized  $\omega$  pulse, the degree of planar alignment  $\langle (\mathbf{e}_y \cdot \mathbf{e}_Y)^2 \rangle$  characterizing the alignment of the molecular plane to the plane defined by the elliptically polarized  $2\omega$  pulse should also be used. It should be noted that  $\langle (\mathbf{e}_z \cdot \mathbf{e}_Z)^2 \rangle$  is equivalent to  $\langle \cos^2 \theta \rangle$  in the present case.

The time evolutions of the above order parameters for iodobenzene molecules are shown in Fig. 6 for case 1 and in Fig. 7 for case 2. We first explore the numerical results obtained under the adiabatic approximation. For given intensities of two-color laser pulses, the highest possible degrees of molecular orientation can be achieved when the molecular orientation dynamics is purely adiabatic. In the case of linearly polarized two-color laser fields with their polarizations crossed obliquely [Fig. 6(a)], although the degree of planar alignment  $\langle (\mathbf{e}_y \cdot \mathbf{e}_Y)^2 \rangle$  increases monotonically, the degrees of molecular alignment and orientation saturate before the peak intensities and slightly decrease toward the peak intensities. This behavior can be understood by referring to Fig. 2. The alignment potential  $\hat{H}_\alpha$ , which dominates the overall shape of the interaction potential as explained above, is the deepest along directions slightly tilted from the vertical  $Z$  axis. Consequently, the degrees of alignment and orientation defined above tend to decrease when the intensities of the laser pulses are high enough. In addition, the actual direction of aligned and oriented molecular ensemble achieved with this conventional approach [30] depends on the contribution of the  $E'_{2\omega}(t)$  component, which is not convenient in experimental implementations and further applications. In contrast, our approach with combined linearly polarized and elliptically polarized pulse [29] ensures that the alignment potential  $\hat{H}_\alpha$  is always the deepest along the vertical  $Z$  axis. Consequently, all of the order parameters increase monotonically till the peak intensities with our approach as shown in Fig. 6(b). More importantly, all of the order parameters at the peak intensities achieved with our approach are higher than those with the linearly polarized two-color laser fields with their polarizations crossed obliquely.

We find that the molecular orientation dynamics is not adiabatic even with longer pulse widths  $\tau_\omega = 12$  ns and  $\tau_{2\omega} = 9$  ns as discussed below. The nonadiabatic behavior must be carefully examined by solving the time-dependent Schrödinger equation. When the molecular orientation dynamics is nonadiabatic, stronger orientation cannot necessarily be achieved simply by increasing the intensities of the two-color laser pulses. Its mechanism can be qualitatively understood as follows: First, it should be noted that in general the pulse width of the  $\omega$  pulse is longer than that of

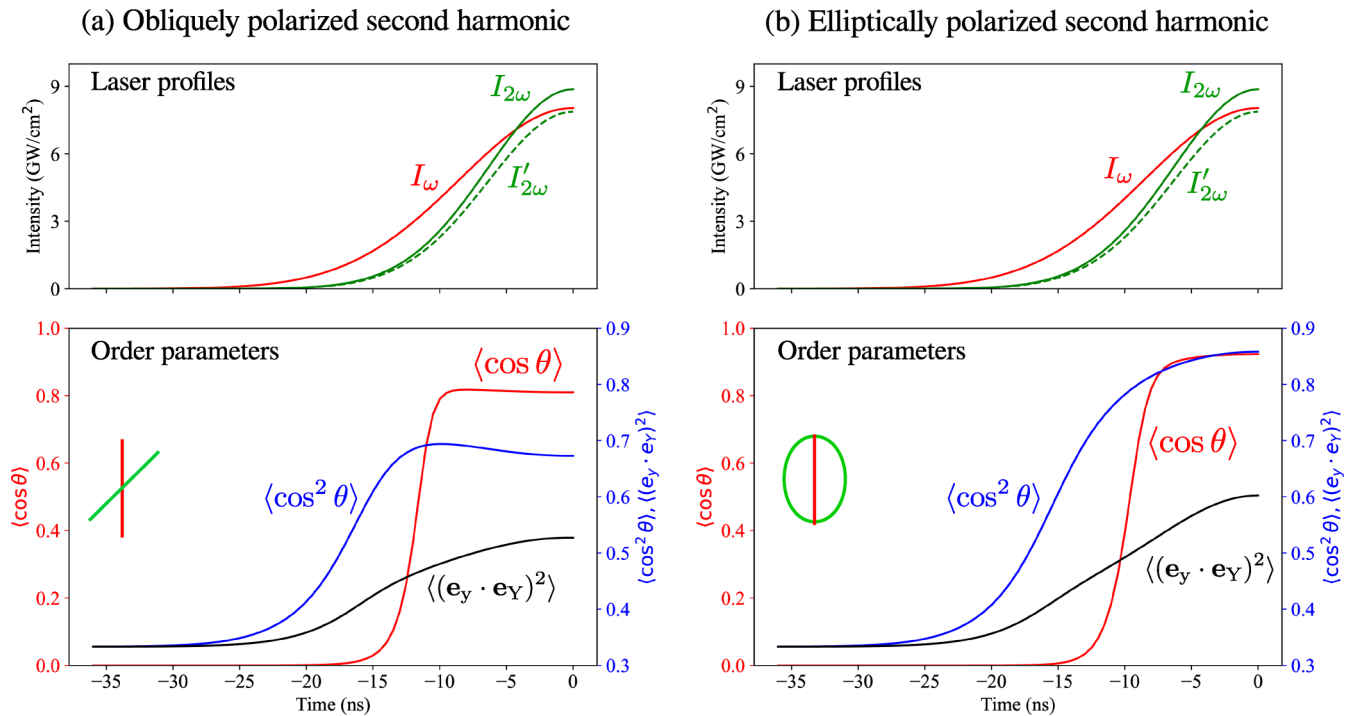


FIG. 6. Degrees of alignment  $\langle \cos^2 \theta \rangle$ , orientation  $\langle \cos \theta \rangle$ , and planar alignment  $\langle (\mathbf{e}_y \cdot \mathbf{e}_Y)^2 \rangle$  of iodobenzene molecules which are initially in their rotational ground state as a function of time on the leading edge of the two-color laser pulses (lower panel), and the intensity profiles of the two-color laser pulses (upper panel). (a) The results obtained for linearly polarized two-color laser fields with their polarizations crossed obliquely. (b) The results obtained for a linearly polarized  $\omega$  pulse and an elliptically polarized  $2\omega$  pulse. The results are obtained by solving the relevant *time-independent* Schrödinger equation under the adiabatic approximation.

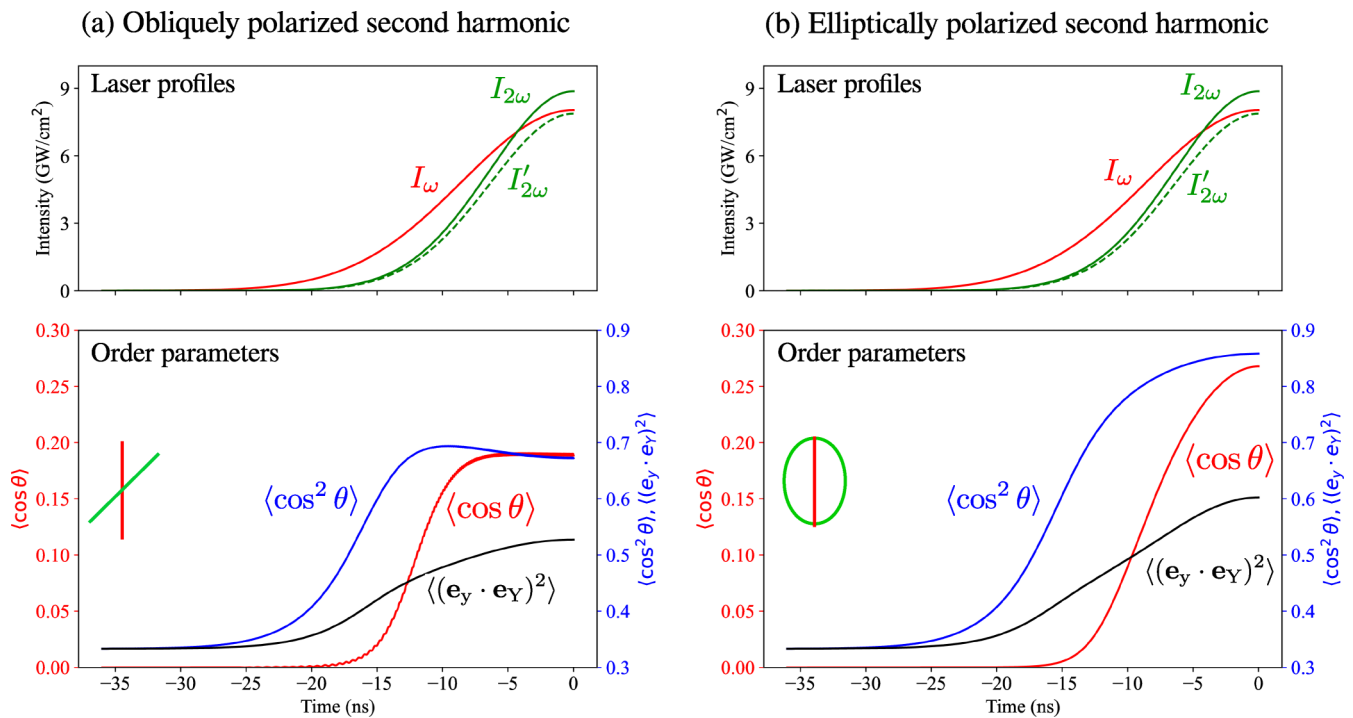


FIG. 7. Degrees of alignment  $\langle \cos^2 \theta \rangle$ , orientation  $\langle \cos \theta \rangle$ , and planar alignment  $\langle (\mathbf{e}_y \cdot \mathbf{e}_Y)^2 \rangle$  of iodobenzene molecules which are initially in their rotational ground state as a function of time on the leading edge of the two-color laser pulses (lower panel), and the intensity profiles of the two-color laser pulses (upper panel). (a) The results obtained for linearly polarized two-color laser fields with their polarizations crossed obliquely. The small ripples visible in the red  $\langle \cos \theta \rangle$  curve are artifacts, which stem from the finite time step in the numerical calculations and have no physical meaning. (b) The results obtained for a linearly polarized  $\omega$  pulse and an elliptically polarized  $2\omega$  pulse. The results are obtained by solving the relevant *time-dependent* Schrödinger equation to examine the nonadiabatic effects.

the  $2\omega$  pulse because of the unsaturated second-harmonic generation process. Since the intensity of the  $\omega$  pulse first starts to increase and the symmetric alignment potential is created, the rotationally excited states are equally distributed in both of the symmetric double-well potentials and only the molecular alignment is created. After a while the intensity of the  $2\omega$  pulse starts to increase, and the asymmetric double-well potential required for molecular orientation is gradually created but the high potential barrier between the double-well potentials mainly created by  $\hat{H}_\alpha$  hampers the tunnel transitions of rotational states from the shallower potential well to the deeper one. Therefore, it is difficult to achieve higher degrees of orientation when the molecular orientation dynamics is nonadiabatic. This serious situation can be significantly mitigated by our approach with a linearly polarized  $\omega$  pulse and an elliptically polarized  $2\omega$  pulse [29]. This is made possible by the suppressed potential barriers along the azimuthal angles  $\phi = 0$  and  $\pi$ , which are created by the elliptically polarized  $2\omega$  pulse as explained above and contribute to the promotion of the tunnel transition from the shallower potential well to the deeper one when the molecular orientation dynamics is nonadiabatic.

Now the validity of our strategy explained above is ascertained by numerical simulations (numerical experiments). The time evolutions of the order parameters obtained by solving the relevant time-dependent Schrödinger equation are shown in Fig. 7. The important features observed in the comparison between Figs. 6 and 7 are as follows.

(1) The degrees of orientation  $\langle \cos \theta \rangle$  in Fig. 7 are lower than those in Fig. 6. This is a clear manifestation that the molecular orientation dynamics is actually nonadiabatic even for longer pulse widths of  $\tau_\omega = 12$  ns and  $\tau_{2\omega} = 9$  ns.

(2) The degree of orientation in Fig. 7(b) is higher than that in Fig. 7(a). Although the same relation is observed between Figs. 6(a) and 6(b), the superiority of our approach over the conventional approach is more prominent in Fig. 7 than in Fig. 6. This means that our approach is more advantageous than the conventional approach especially when the molecular orientation dynamics is nonadiabatic.

(3) The degrees of alignment  $\langle \cos^2 \theta \rangle$  and planar alignment  $\langle (\mathbf{e}_y \cdot \mathbf{e}_Y)^2 \rangle$  in Fig. 7 are the same as those in Fig. 6. This means that the alignment dynamics and the planar alignment dynamics are adiabatic for the pulse widths of  $\tau_\omega = 12$  ns and  $\tau_{2\omega} = 9$  ns. In the case of alignment, there is no need for the tunnel transitions from the shallower potential well to the deeper one. On the other hand, for achieving molecular orientation, our result demonstrates that two-color pulses with the pulse widths longer than 12 and 9 ns are necessary to ensure the adiabatic orientation. The necessity of the longer pulse widths for achieving the adiabatic molecular orientation is explained by the smaller energy differences among the relevant rotational quantum states in the sample molecules, and the necessary pulse widths are roughly determined by the uncertainty principle.

## V. SUMMARY AND OUTLOOK

Our approach with a linearly polarized  $\omega$  pulse and an elliptically polarized  $2\omega$  pulse for achieving molecular orientation has been originally proposed to achieve higher degrees

of orientation when the molecular orientation dynamics is nonadiabatic and its validity has been numerically demonstrated for achieving one-dimensional molecular orientation [29]. In this paper, we have successfully demonstrated that our approach can be naturally extended to achieve three-dimensional molecular orientation because of the usage of an elliptically polarized  $2\omega$  pulse. That is, all the three order parameters to characterize three-dimensional molecular orientation can be successfully controlled with our approach.

Here we summarize our findings.

(1) The molecular orientation dynamics is actually nonadiabatic even for longer pulse widths of  $\tau_\omega = 12$  ns and  $\tau_{2\omega} = 9$  ns.

(2) Our approach is more advantageous than the conventional approach with linearly polarized two-color pulses with their polarizations crossed obliquely especially when the molecular orientation dynamics is nonadiabatic.

(3) In contrast to the molecular orientation dynamics, the alignment dynamics and the planar alignment dynamics are adiabatic, from the viewpoint of their order parameters, for the pulse widths of  $\tau_\omega = 12$  ns and  $\tau_{2\omega} = 9$  ns.

In addition to the experimental realization of one- and three-dimensional molecular orientation with our own approach, completely field-free one- and three-dimensional molecular orientation is a remaining future subject. This will be made possible by turning off the intense nanosecond two-color laser pulses at their peak intensities rapidly within  $\approx 150$  fs by applying a plasma shutter. An indispensable prerequisite for such a plasma shutter is to stabilize the relative phase difference between the two wavelengths. Such a plasma shutter is now being developed in our group.

A sample of three-dimensionally aligned and oriented molecules is an ideal anisotropic quantum system for many research fields in electronic stereodynamics in molecules [1] as well as stereodynamics in chemical reactions. Especially, the preparation of an ensemble of three-dimensionally oriented molecules is prerequisite to prepare one of the enantiomers from the 50:50 racemate [38,39].

## ACKNOWLEDGMENTS

The authors thank Dr. Shinichirou Minemoto, Mr. Takakuni Fukumoto, and Mr. Naoki Hara for their fruitful discussions.

## APPENDIX: MATRIX ELEMENTS USED IN THE INTERACTION POTENTIALS (HAMILTONIANS) IN TERMS OF WIGNER $D$ MATRICES

To run numerical simulations, a wave function  $|\Psi(t)\rangle$  is expanded in terms of symmetric-top wave functions  $|JKM\rangle$  as given by Eq. (A1):

$$|JKM\rangle = \left[ \frac{2J+1}{8\pi^2} \right]^{\frac{1}{2}} D_{MK}^{J*}(\phi, \theta, \chi), \quad (\text{A1})$$

where  $D_{MK}^{J*}(\phi, \theta, \chi)$  is the complex conjugate of the Wigner  $D$  matrix  $D_{MK}^J(\phi, \theta, \chi)$ . The matrix elements used in the interaction potentials (Hamiltonians) of Eqs. (4)–(6) and (7)–(9)



are calculated by the following equation [32]:

$$\begin{aligned} & \langle J'K'M' | D_{M_0K_0}^{J_0} | JKM \rangle \\ &= (-1)^{M-K} \sqrt{(2J'+1)(2J+1)} \\ & \times \begin{pmatrix} J & J_0 & J' \\ -M & M_0 & M' \end{pmatrix} \begin{pmatrix} J & J_0 & J' \\ -K & K_0 & K' \end{pmatrix}. \end{aligned} \quad (\text{A2})$$

The trigonometric functions of  $\phi$ ,  $\theta$ , and  $\chi$  in Eqs. (4)–(6) and (7)–(9) have to be expressed in terms of the Wigner  $D$  matrix  $D_{MK}^J(\phi, \theta, \chi)$  before we can use (A2) to find out the necessary matrix elements corresponding to these terms. The Wigner  $D$ -matrix representations of these functions are calculated using the tables given in Refs. [32,40] and are summarized as follows:

$$\cos\theta = D_{00}^1, \quad (\text{A3})$$

$$\cos^2\theta = \frac{1}{3} + \frac{2}{3}D_{00}^2, \quad (\text{A4})$$

$$\cos^3\theta = \frac{2}{5}D_{00}^3 + \frac{3}{5}D_{00}^1, \quad (\text{A5})$$

$$\cos^2\phi\sin^2\theta = \frac{1}{3} - \frac{1}{3}D_{00}^2 + \frac{1}{\sqrt{6}}D_{20}^2 + \frac{1}{\sqrt{6}}D_{-20}^2, \quad (\text{A6})$$

$$\sin^2\theta\cos^2\chi = \frac{1}{3} - \frac{1}{3}D_{00}^2 + \frac{1}{\sqrt{6}}D_{02}^2 + \frac{1}{\sqrt{6}}D_{0-2}^2, \quad (\text{A7})$$

$$\cos\phi\cos\theta\sin\theta = \frac{1}{\sqrt{6}}D_{-10}^2 - \frac{1}{\sqrt{6}}D_{10}^2, \quad (\text{A8})$$

$$\begin{aligned} \cos\phi\cos^2\theta\sin\theta &= \frac{2}{5\sqrt{3}}D_{-10}^3 - \frac{2}{5\sqrt{3}}D_{10}^3 \\ &+ \frac{\sqrt{2}}{10}D_{-10}^1 - \frac{\sqrt{2}}{10}D_{10}^1, \end{aligned} \quad (\text{A9})$$

$$\begin{aligned} (\mathbf{e}_y \cdot \mathbf{e}_Y)^2 &= (-\sin\phi\cos\theta\sin\chi + \cos\phi\cos\chi)^2 \\ &= \frac{1}{3} + \frac{1}{6}D_{00}^2 + \frac{1}{4}D_{-2-2}^2 + \frac{1}{4}D_{22}^2 + \frac{1}{4}D_{2-2}^2 \\ &+ \frac{1}{4}D_{-22}^2 + \frac{1}{2\sqrt{6}}D_{-20}^2 + \frac{1}{2\sqrt{6}}D_{0-2}^2 \\ &+ \frac{1}{2\sqrt{6}}D_{20}^2 + \frac{1}{2\sqrt{6}}D_{02}^2, \end{aligned} \quad (\text{A10})$$

$$\begin{aligned} & (\cos\phi\cos\theta\cos\chi - \sin\phi\sin\chi)^2 \\ &= \frac{1}{3} + \frac{1}{6}D_{00}^2 + \frac{1}{4}D_{-2-2}^2 + \frac{1}{4}D_{22}^2 + \frac{1}{4}D_{2-2}^2 + \frac{1}{4}D_{-22}^2 \\ &- \frac{1}{2\sqrt{6}}D_{-20}^2 - \frac{1}{2\sqrt{6}}D_{0-2}^2 - \frac{1}{2\sqrt{6}}D_{20}^2 - \frac{1}{2\sqrt{6}}D_{02}^2, \end{aligned} \quad (\text{A11})$$

$$\begin{aligned} & \sin\theta\cos\chi(\cos\phi\cos\theta\cos\chi - \sin\phi\sin\chi) \\ &= -\frac{1}{4}D_{-1-2}^2 - \frac{1}{4}D_{-12}^2 + \frac{1}{2\sqrt{6}}D_{-10}^2 - \frac{1}{2\sqrt{6}}D_{10}^2 \\ &+ \frac{1}{4}D_{1-2}^2 + \frac{1}{4}D_{12}^2, \end{aligned} \quad (\text{A12})$$

$$\cos\theta\sin^2\theta\cos^2\chi = \frac{1}{5}D_{00}^3 - \frac{1}{5}D_{00}^1 + \frac{1}{\sqrt{30}}D_{0-2}^3 + \frac{1}{\sqrt{30}}D_{02}^3, \quad (\text{A13})$$

$$\cos\theta\sin^2\theta\sin^2\chi = \frac{1}{5}D_{00}^3 - \frac{1}{5}D_{00}^1 - \frac{1}{\sqrt{30}}D_{0-2}^3 - \frac{1}{\sqrt{30}}D_{02}^3, \quad (\text{A14})$$

$$\begin{aligned} & \cos\phi\sin\theta(1 - 3\cos^2\theta)\cos^2\chi + \sin\phi\cos\theta\sin\theta\sin 2\chi \\ &= \frac{1}{\sqrt{10}}D_{-1-2}^3 + \frac{1}{\sqrt{10}}D_{-12}^3 - \frac{1}{\sqrt{10}}D_{1-2}^3 - \frac{1}{\sqrt{10}}D_{12}^3 \\ &+ \frac{\sqrt{2}}{10}D_{-10}^1 - \frac{\sqrt{2}}{10}D_{10}^1 - \frac{\sqrt{3}}{5}D_{-10}^3 + \frac{\sqrt{3}}{5}D_{10}^3, \end{aligned} \quad (\text{A15})$$

$$\begin{aligned} & \cos\phi\sin\theta(1 - 3\cos^2\theta)\sin^2\chi - \sin\phi\cos\theta\sin\theta\sin 2\chi \\ &= -\frac{1}{\sqrt{10}}D_{-1-2}^3 - \frac{1}{\sqrt{10}}D_{-12}^3 + \frac{1}{\sqrt{10}}D_{1-2}^3 + \frac{1}{\sqrt{10}}D_{12}^3 \\ &+ \frac{\sqrt{2}}{10}D_{-10}^1 - \frac{\sqrt{2}}{10}D_{10}^1 - \frac{\sqrt{3}}{5}D_{-10}^3 + \frac{\sqrt{3}}{5}D_{10}^3. \end{aligned} \quad (\text{A16})$$

- 
- [1] D. Herschbach, Chemical stereodynamics: Retrospect and prospect, *Eur. Phys. J. D* **38**, 3 (2006).
- [2] M. Lemeshko, R. V. Krems, J. M. Doyle, and S. Kais, Manipulation of molecules with electromagnetic fields, *Mol. Phys.* **111**, 1648 (2013).
- [3] C. P. Koch, M. Lemeshko, and D. Sugny, Quantum control of molecular rotation, *Rev. Mod. Phys.* **91**, 035005 (2019).
- [4] Y. Fujimura and H. Sakai, *Electronic and Nuclear Dynamics in Molecular Systems* (World Scientific, Singapore, 2011), Chap. 4.
- [5] I. V. Litvinyuk, K. F. Lee, P. W. Dooley, D. M. Rayner, D. M. Villeneuve, and P. B. Corkum, Alignment-dependent strong field ionization of molecules, *Phys. Rev. Lett.* **90**, 233003 (2003).
- [6] D. Zeidler, A. Staudte, A. B. Bardon, D. M. Villeneuve, R. Dörner, and P. B. Corkum, Controlling attosecond double ionization dynamics via molecular alignment, *Phys. Rev. Lett.* **95**, 203003 (2005).
- [7] T. Suzuki, S. Minemoto, T. Kanai, and H. Sakai, Optimal control of multiphoton ionization processes in aligned  $I_2$  molecules with time-dependent polarization pulses, *Phys. Rev. Lett.* **92**, 133005 (2004).
- [8] T. Kanai, S. Minemoto, and H. Sakai, Quantum interference during high-order harmonic generation from aligned molecules, *Nature (London)* **435**, 470 (2005).
- [9] T. Kanai, S. Minemoto, and H. Sakai, Ellipticity dependence of high-order harmonic generation from aligned molecules, *Phys. Rev. Lett.* **98**, 053002 (2007).

- [10] K. Nakajima, T. Teramoto, H. Akagi, T. Fujikawa, T. Majima, S. Minemoto, K. Ogawa, H. Sakai, T. Togashi, K. Tono, S. Tsuru, K. Wada, M. Yabashi, and A. Yagishita, Photoelectron diffraction from laser-aligned molecules with x-ray free-electron laser pulses, *Sci. Rep.* **5**, 14065 (2015).
- [11] S. Minemoto, T. Teramoto, H. Akagi, T. Fujikawa, T. Majima, K. Nakajima, K. Niki, S. Owada, H. Sakai, T. Togashi, K. Tono, S. Tsuru, K. Wada, M. Yabashi, S. Yoshida, and A. Yagishita, Structure determination of molecules in an alignment laser field by femtosecond photoelectron diffraction using an x-ray free-electron laser, *Sci. Rep.* **6**, 38654 (2016).
- [12] J. H. Mun, S. Minemoto, D. E. Kim, and H. Sakai, All-optical control of pendular qubit states with nonresonant two-color laser pulses, *Commun. Phys.* **5**, 226 (2022).
- [13] B. Friedrich and D. Herschbach, Enhanced orientation of polar molecules by combined electrostatic and nonresonant induced dipole forces, *J. Chem. Phys.* **111**, 6157 (1999).
- [14] B. Friedrich and D. Herschbach, Manipulating molecules via combined static and laser fields, *J. Phys. Chem. A* **103**, 10280 (1999).
- [15] H. Sakai, S. Minemoto, H. Nanjo, H. Tanji, and T. Suzuki, Controlling the orientation of polar molecules with combined electrostatic and pulsed, nonresonant laser fields, *Phys. Rev. Lett.* **90**, 083001 (2003).
- [16] S. Minemoto, H. Nanjo, H. Tanji, T. Suzuki, and H. Sakai, Observation of molecular orientation by the combination of electrostatic and nonresonant, pulsed laser fields, *J. Chem. Phys.* **118**, 4052 (2003).
- [17] H. Tanji, S. Minemoto, and H. Sakai, Three-dimensional molecular orientation with combined electrostatic and elliptically polarized laser fields, *Phys. Rev. A* **72**, 063401 (2005).
- [18] A. Goban, S. Minemoto, and H. Sakai, Laser-field-free molecular orientation, *Phys. Rev. Lett.* **101**, 013001 (2008).
- [19] J. H. Mun, D. Takei, S. Minemoto, and H. Sakai, Laser-field-free orientation of state-selected asymmetric top molecules, *Phys. Rev. A* **89**, 051402(R) (2014).
- [20] D. Takei, J. H. Mun, S. Minemoto, and H. Sakai, Laser-field-free three-dimensional molecular orientation, *Phys. Rev. A* **94**, 013401 (2016).
- [21] T. Kanai and H. Sakai, Numerical simulations of molecular orientation using strong, nonresonant, two-color laser fields, *J. Chem. Phys.* **115**, 5492 (2001).
- [22] K. Oda, M. Hita, S. Minemoto, and H. Sakai, All-optical molecular orientation, *Phys. Rev. Lett.* **104**, 213901 (2010).
- [23] M. M. Hossain, X. Zhang, S. Minemoto, and H. Sakai, Stronger orientation of state-selected OCS molecules with relative-delay-adjusted nanosecond two-color laser pulses, *J. Chem. Phys.* **156**, 041101 (2022).
- [24] Y. Sugawara, A. Goban, S. Minemoto, and H. Sakai, Laser-field-free molecular orientation with combined electrostatic and rapidly-turned-off laser fields, *Phys. Rev. A* **77**, 031403(R) (2008).
- [25] M. Muramatsu, M. Hita, S. Minemoto, and H. Sakai, Field-free molecular orientation by an intense nonresonant two-color laser field with a slow turn on and rapid turn off, *Phys. Rev. A* **79**, 011403(R) (2009).
- [26] S. Minemoto, W. Komatsubara, and H. Sakai, Comparative studies of the degrees of orientation of CO molecules pumped by intense femtosecond two-color pulses based on high-order harmonic generation and Coulomb explosion imaging, *J. Phys. B* **53**, 235101 (2020).
- [27] J. H. Mun and H. Sakai, Improving molecular orientation by optimizing relative delay and intensities of two-color laser pulses, *Phys. Rev. A* **98**, 013404 (2018).
- [28] J. H. Mun, H. Sakai, and R. González-Férez, Orientation of linear molecules in two-color laser fields with perpendicularly crossed polarizations, *Phys. Rev. A* **99**, 053424 (2019).
- [29] M. M. Hossain and H. Sakai, All-optical orientation of linear molecules with combined linearly and elliptically polarized two-color laser fields, *J. Chem. Phys.* **153**, 104102 (2020).
- [30] N. Takemoto and K. Yamanouchi, Fixing chiral molecules in space by intense two-color phase-locked laser fields, *Chem. Phys. Lett.* **451**, 1 (2008).
- [31] K. Lin, I. Tutunnikov, J. Qiang, J. Ma, Q. Song, Q. Ji, W. Zhang, H. Li, F. Sun, X. Gong, H. Li, P. Lu, H. Zeng, Y. Prior, I. S. Averbukh, and J. Wu, All-optical field-free three-dimensional orientation of asymmetric-top molecules, *Nat. Commun.* **9**, 5134 (2018).
- [32] R. N. Zare, *Angular Momentum: Understanding Spatial Aspects in Chemistry and Physics* (Wiley, New York, 1988).
- [33] H. Nakabayashi, W. Komatsubara, and H. Sakai, Recipe for preparing a molecular ensemble with macroscopic threefold symmetry, *Phys. Rev. A* **99**, 043420 (2019).
- [34] D. Mellado-Alcedo, N. R. Quintero, and R. González-Férez, Linear polar molecule in a two-color cw laser field: A symmetry analysis, *Phys. Rev. A* **102**, 023110 (2020).
- [35] N. Matsuzawa and D. A. Dixon, Density functional theory predictions of polarizabilities and first- and second-order hyperpolarizabilities for molecular systems, *J. Phys. Chem.* **98**, 2545 (1994).
- [36] O. Dorosh, E. Białkowska-Jaworska, Z. Kisiel, and L. Piszczółkowski, New measurements and global analysis of rotational spectra of Cl-, Br-, and I-benzene: Spectroscopic constants and electric dipole moments, *J. Mol. Spectrosc.* **246**, 228 (2007).
- [37] J. L. Neill, S. T. Shipman, L. Alvarez-Valtierra, A. Lesarri, Z. Kisiel, and B. H. Pate, Rotational spectroscopy of iodobenzene and iodobenzene-neon with a direct digital 2–8 GHz chirped-pulse Fourier transform microwave spectrometer, *J. Mol. Spectrosc.* **269**, 21 (2011).
- [38] Y. Fujimura, L. González, K. Hoki, J. Manz, and Y. Ohtsuki, Selective preparation of enantiomers by laser pulses: Quantum model simulation for H<sub>2</sub>POSH, *Chem. Phys. Lett.* **306**, 1 (1999).
- [39] K. Hoki, Y. Ohtsuki, and Y. Fujimura, Locally designed pulse shaping for selective preparation of enantiomers from their racemate, *J. Chem. Phys.* **114**, 1575 (2001).
- [40] Y. Chiu, Quantum theory of interference and polarization of Stark-Zeeman lines in molecules, *J. Chem. Phys.* **45**, 2969 (1966).